J Braz. Soc. Mech. Sci. Eng. (2017) 39:5195–5204
https://doi.org/10.1007/s40430-017-0904-8

TECHNICAL PAPER

Prediction of the convective heat transfer coefficient of cutting fluid in helical drills

Douglas Wellington Pontes[1] · Joel Martins Crichigno Filho[1] · Paulo Sérgio Berving Zdanski[1]

Received: 27 April 2017 / Accepted: 28 August 2017 / Published online: 8 September 2017

Abstract Environmental, economical and social factors impose the elimination or reduction of the quantity of the cutting fluids used in the machining. This trend leads to a high temperature in the cutting zone. In drilling, when the cutting fluid is not supplied through the spindle, the tool tip suffers from high temperature, leading to rapid wear. In this case, the cooling of the drill tool body can contribute significantly removing the heat generated at the tool–chip interface. However, to effectively simulate the temperature at the tool tip, the effect of the cutting fluid on tool body must be known. Hence, the aim of this work was to determine the convective heat transfer coefficient of the cutting fluid on the complex body of a helical drill. In this regard, a special experimental setup is developed, allowing the drill to remain static while the coolant nozzle rotates around providing cutting fluid. A method is developed in order to determine the temperature on the drill surface as a function of the heat enters into the drill and the temperature measured at the tool base. Experiments are carried out varying coolant nozzle rotation speed and the cutting fluid flow rate. According to the results, the cutting fluid flow rate shows to have the most significant effect on the convective heat transfer coefficient.

Technical Editor: Márcio Bacci da Silva.

✉ Joel Martins Crichigno Filho
joel.crichigno@udesc.br

Douglas Wellington Pontes
dougv8.247@gmail.com

Paulo Sérgio Berving Zdanski
paulo.zdanski@udesc.br

[1] Department of Mechanical Engineering, Santa Catarina State University, Campus Universitario, Joinville 89219-710, Brazil

Keywords Cutting fluid · Convective heat transfer · Temperature · Drilling

List of symbols

∇	Laplace operator vector
A_2	Contact area of the drill with the cutting fluid (m^2)
A_b	Surface back area of the heating system (m^2)
A_f	front surface area of the heating system (m^2)
$A_{1,3}$	Cross-sectional area of the drill (m^2)
$E_{f,t,l}$	Insulation thickness (m)
h	Convective heat transfer coefficient (W/m^2 K)
I	Current (A)
k	Thermal conductivity of the tool material (W/mK)
k_i	Thermal conductivity of the insulation (W/mK)
L	Insulation length (m)
l_f	Cutting fluid flow rate (l/h)
Q_d	Heat entering the drill (W)
Q_f	Heat removed by the cutting fluid (W)
Q_r	Heat supplied by the electric resistance (W)
$Q_{l1\ldots l3}$	Heat lost at the heating system (W)
R_n	Nozzle rotating speed (rpm)
$R_{1\ldots4}$	Regions of the drill (rpm)
$r_{e,i}$	Insulation radius (m)
$S_{1,2,3}$	Surfaces of the drill (m^2)
T	Temperature in the drill (°C)
$T_1 \ldots T_5$	Temperatures inside the heating system (°C)
T_a	Room temperature (°C)
T_d	Temperature on the drill surface (°C)
T_f	Cutting fluid temperature (°C)
T_{b1}	Temperature on the surface A_3 (°C)
T_{b2}	Temperature on the back of the tool (°C)
U	Voltage (V)
$VC_1, 2$	Control volume

1 Introduction

Drilling is a manufacturing process widely used to produce holes in mechanical components of various sizes and depths. Since the tool is constrained in a hole, the tool temperature tends to be higher than in other processes under similar conditions. The high temperature at the tool tip has a great influence on the tool life and surface quality [1]. In order to provide cooling and lubrication, cutting fluids should be applied. The most common approach is the flooding by means of a nozzle system. A great amount of cutting fluid is delivered on the tool and workpiece without control of flow rate and volume. Despite this, the counterflow of the chips inhibits the fluid to reach the drill tip Fig. 1.

The external supply of the cutting fluid is, therefore, less effective. The through-tool coolant system allows the cutting fluid to reach the tool tip through the cutting tool flank. Hence, this method is more effective. On the other hand, the machine tool need to be designed to deliver coolant through the spindle and tool directly to the cutting interface, which makes the machine to be more expensive. Due to the fact that the use of cutting fluids results in negative impacts on environment, safety, operators health, and operating cost, its the minimisation or even elimination is a strong global trend [2]. New technologies have emerged in order to minimise the impact of cutting fluids. One such technique is the application of minimal quantity of lubricant (MQL), in which the cooling media is supplied as a mixture of air and oil in the form of aerosol [3, 4].

The flow rate applied by MQL is in the order of hundreds of 50 ml/h up to 1–2 l/h, while in flooding the cutting fluid is provided at 10–100 l/min. Therefore, a significant reduction is observed compared to the amount commonly used in flood cooling condition [5, 6]. Due to the fact that MQL applies only a fine mist of air–fluid mixture to the cutting zone, the capacity to carry away heat and providing adequate lubrication is limited [7]. Furthermore, during the drilling the aerosol does not reach the tool tip for the same reasons as the mentioned for the flooding.

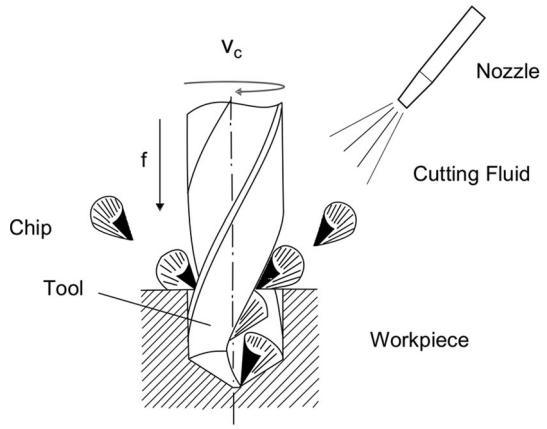

Fig. 1 A schematic representation of the drilling process

From the point of view of minimising the use of cutting fluid, the most effective method is machining without its application, or otherwise known as dry machining. Since, the temperature that is generated at the tool tip can reach above 900 °C without cooling [8–11], the tool wear increases quickly.

In some cases, good results are observed in the dry machining or with application of MQL [12]. In others, the flood coolant supply with environmentally friendly cutting fluids can be an alternative. Mineral-based cutting fluids are still the most used by the industry. This is because of its high lubrication quality, stability and protection against corrosion. However, they are hazardous for storage and disposal and require a special physical or chemical treatment with the objective of environmental protection. Hence, new environmentally friendly cutting fluids are arriving in the market. As an alternative to mineral-based fluids the demand for biodegradable cutting fluids is stimulating the development of vegetable oils [12].

Even, applying a environmentally friendly media, its efficiency in the machining process needs to be maximised. This means that the amount of cutting fluids used in machining must be minimised, while achieving the requirements in terms of tool wear and workpiece quality. In this way, the determination of the correct amount of cutting fluid in each machining process has become of great interest in industry. For instance, Bacci da Silva and Wallbank [13] pointed out the need of the reduction of the volume cutting fluid in machining in the point of view of lubrication effect. The authors argued that "Even if lubrication of the rake face was possible, the volume of cutting fluid applied in practical operations is much higher than the amount necessary to lubricate a small area". Denkena et al. [14] investigated the influence of the coolant flow rate on the tool wear for turning, drilling and milling for different cutting conditions. They optimised the volume flow rate of the coolant in order to maximise tool life. Jiang et al. [15] studied the optimisation of the cutting parameters in turning in order to minimise the cutting fluid consumption and process cost. They carried out practical experiments and applied a multi-objective optimisation model.

Since the temperature at the tool tip is related to the tool wear, the minimal volume flow rate of coolant should be determined in order to maintain the temperature under a certain value. In this respect, the simulation by finite elements plays an important role in the prediction of the temperature at the drill tip [16–18]. For the correct simulation of temperature distribution, the convective heat transfer coefficient of the cutting fluid

on the surface of the cutting tool needs to be determined. Investigation of the heat transfer performance for different cutting fluids and application methods has been investigated by different authors. Daniel et al. [19] studied the heat transfer performance of different cutting fluids in turning and boring in flood and jet application. Li and Shih [16] simulated the temperature distributions at the drill tip by combining finite element thermal model with an inverse heat transfer method. The authors also calculated the convective heat transfer coefficient using the inverse heat transfer solution. The cutting fluid was supplied internally because the drill was static and does not rotate in the experiment. Kops and Arenson [20] presented a numerical iterative procedure to determine the convective heat transfer coefficient for cooling of a rotating cylindrical workpiece in air using a water-based coolant. Sales et al. [21] investigated the cooling ability of the cutting fluids in turning by using different convective heat transfer coefficients. The cooling ability of six different cooling media: atmospheric air, water, integral neat oil, emulsion of soluble oil and two different synthetic fluids was determined. Luchesi and Coelho [22] carried out experiments to estimate the convective heat transfer of cutting fluids in a laminar flow regime. Dry, flooded, and minimum quantity of lubrication cooling methods were compared. Li and Shih [23] pointed out that most of the drill thermal analyses by previous researchers were conducted under dry conditions. That is because temperature is measured using embedded wire thermocouples in the drill tool and hence the tool cannot rotate. In experiments with static drills, the heat transfer between the cutting fluid and the tool body differs from the real situation where the drill rotates. This occurs because the complexity of the geometry of the drill flute profile changes the fluid flow behaviour.

To the best of our knowledge, no research publication is available on the analysis of convective heat transfer coefficient of the cutting fluid with the tool body. In that way, the main objective of this work is to predict the convective heat transfer coefficient of the cutting fluids for a rotating drill tool. The methodology employed to reach this goal is as follows: (1) devise an experimental apparatus for measuring the heat transfer rate and temperature at the drill tool cross section; (2) solve numerically a direct heat conduction problem subjected to boundary conditions evaluated experimentally; (3) obtain the average temperature in the tool surface exposed to forced convection with the cutting fluid and (4) finally to find the convective heat transfer coefficient using the Newton's law of cooling.

2 Problem formulation

During the drilling, the heat exchange can be idealised in four regions, as shown in Fig. 2.

In the first region, the drill tool is inside the hole, removing material from the workpiece. The heat flows to the drill due to (1) the cutting of material at the tool tip, (2) the friction between the drill body and the hole wall and (3) the contact of the chips with the tool flutes. In the second region the drill tool is in contact with the cutting fluid and hence the greatest amount of heat is removed. Heat exchange with air takes place in the third region, but only a small amount is removed. In the last region, the tool transfers heat by conduction to the tool clamping system. Here it is also expected an exchange of a small amount of heat.

As drilling progresses, the cutting depth increases, increasing the heat transfer area between drill and workpiece with a consequent reduction of the exchange region with air. In this work, the region of interest is the part of the drill that exchanges heat by convection with the cutting fluid, i.e., the second region described above.

This region can be modelled according to the control volume VC_1 shown in Fig. 3.

The heat flowing into the control volume VC_1 is Q_d. The amount of heat removed by the fluid is Q_f. The differential energy equation is used to obtain the steady-state temperature distribution in the drill tool (VC_1)

$$\nabla \bullet (k\ \nabla T) = 0, \tag{1}$$

where ∇ is the Nabla operator and k is the thermal conductivity of the drill material. The Eq. 1 was solved numerically subjected to the following boundary conditions:

- On the surface where the heat enters the drill:

$$A_1\, k\, \frac{\partial T}{\partial S}\bigg|_{S=S_1} = Q_d. \tag{2}$$

- On the surface where the drill tool exchanges heat with the cutting fluid:

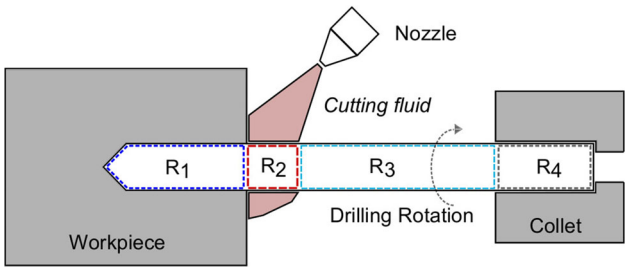

Fig. 2 Modelling of drill tool in four different regions

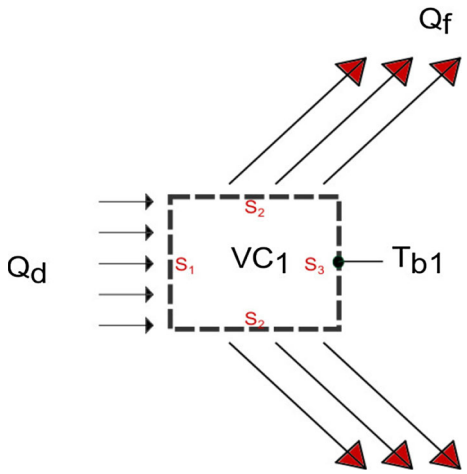

Fig. 3 Energy balance in control volume VC_1

$$A_2\, k \left.\frac{\partial T}{\partial S}\right|_{S=S_2} = -Q_\mathrm{f}, \tag{3}$$

where A_1 is the cross-sectional area of the drill and A_2 is the contact area of the drill with the fluid.

To solve Eq. (1) it is necessary to know the thermal condition at surface S_3 shown in Fig. 3. Therefore, the following boundary condition is assumed:

- The prescribed temperature on the surface A_3 is as follows:

$$T\Big|_{S=S_3} = T_{b1} \tag{4}$$

Thus, Eq. (1) can be solved with the boundary conditions (2), (3) and (4) to calculate the temperature distribution at the drill–cutting fluid interface. It is important to mention that in steady-state condition it is expected that all the heat transferred to the drill is exchanged with cutting fluid; therefore, $Q_\mathrm{f} = Q_\mathrm{d}$. In this case, the temperature of the drill base T_{b1} must remain constant.

The mean temperature at the drill surface in contact with the cutting fluid is calculated as

$$T_\mathrm{d} = \frac{1}{A_2}\int_{A_2} T\,\mathrm{d}A \tag{5}$$

Once the mean temperature on the drill surface T_d is found, the mean convective heat transfer coefficient is determined by

$$h = \frac{Q_\mathrm{f}}{A_2(T_d - T_f)}, \tag{6}$$

where A_2 is the area of the drill that exchanges heat with the cutting fluid and T_f is the temperature of the cutting fluid.

In this way, the convective heat transfer coefficient h can be determined by knowing the heat flux Q_d entering into the control volume VC_1 and measuring the temperature T_{b1} in the control volume VC_2.

Finally, all the procedures followed for obtained the convective heat transfer coefficient may be summarised: (1) obtain experimentally the heat flux Q_d entering into the control volume VC_1 and the temperature T_{b1} in the tool base; (2) obtain numerically the temperature distribution inside the drill tool solving Eqs. (1)–(4); (3) evaluate numerically the average temperature in the tool surface with Eq. (5); (4) obtain the surface area of the drill A_2 using the CAD model; (5) obtain the convective coefficient applying the Newton's law of cooling, Eq. (6).

The numerical-experimental procedure consists of the following sequence:

1. Determine experimentally the heat flux Q_d for the drill and the temperature at the back of the tool T_{b2};
2. simulate the temperature distribution at the drill surface that is in contact with the cutting fluid;
3. calculate the mean temperature at the drill surface T_d for the boundary conditions (2);
4. with T_d and the temperature of the cutting fluid T_f solve Eq. (6), to obtain the mean value of the convective heat transfer coefficient h.

3 Experimental setup

A dedicated experimental setup is developed. It consists basically of heating, insulation and supply of cutting fluid systems. Figure 4 shows a schematic drawing of the experimental setup used in this work.

In the heating system, an electric resistance heats a steel SAE 1020 core, in which the drill tip is inserted. Thermal paste is applied between the core and the drill tool in order

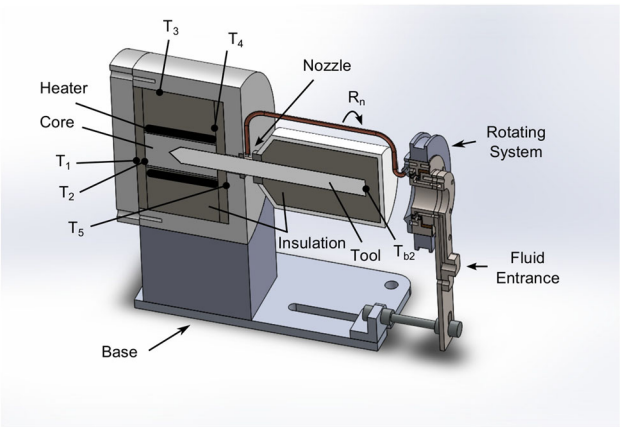

Fig. 4 Experimental setup

to increase heat transfer. The set is enclosed in a refractory cement casing and between them layers of thermal insulation material are used in order to minimise the heat losses. The heating power is adjusted using a TRIAC dimmer.

A 20 mm diameter and 205 mm length drill tool is used in the experiments. The drill is inserted 105 mm into the heating system. To facilitate the analysis, only a small part is cooled by the cutting fluid, circa of 10 mm.

A cooling system with a rotary nozzle is developed to mimic the rotation movement of the drill. With that, the tool remains static, while the nozzle rotates around the tool. A rotating seal permits that the fluid flows to the rotor, where a 3-mm internal diameter copper tube is connected, transporting cutting fluid up to the nozzle. Power is transmitted to the rotor by a belt drive using a DC motor, which is controlled by means of a potentiometer. The speed of rotation is adjusted using a tachometer. The fluid applied to cool the drill surface is collected in a plastic tank.

The prediction of the temperature T_{b1} in the control volume VC_1 should be performed in the centre of the drill. However, the insertion a thermocouple can disrupt the experiments. Hence, the temperature T_{b2} is measured at the back of the tool. By isolating the part of drill corresponding to the control volume VC_2 guarantees that no heat is exchanged with the environment, and the temperature T_{b1} is equal to T_{b2}.

Figure 5 shows the model including the control volumes VC_1 and VC_2, i.e. the regions where heat exchange with the cutting fluid occurs and the insulated part of the drill.

For data acquisition, a PC computer connected with a thermocouple module SCXI-1100 from National Instruments is used. Data acquisition is performed by Labview at a rate of 1 Hz. The data are stored to be processed off-line. Eight *K*-type thermocouples are used to measure the temperatures. The cutting fluid temperature T_f, the room temperature T_a, the temperature at the back of the tool T_{b2} are measured. Five thermocouples (T_1–T_5) are used to account for the actual amount of heat transferred to the drill.

The heat Q_d flowing into the drill is calculated according to the energy balance in the control volume VC_1, Eq. (7).

$$Q_d = Q_r - Q_{l1} - Q_{l2} - Q_{l3}, \tag{7}$$

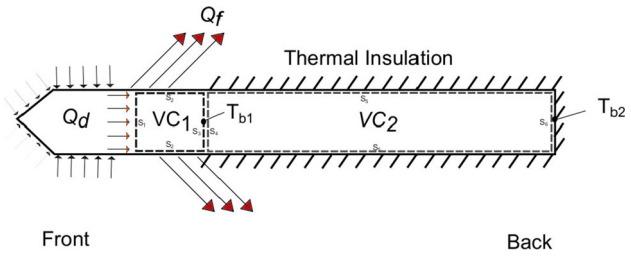

Fig. 5 Energy balance in control volume VC_1 and VC_2

where Q_d is the heat that enters in the drill, Q_r is the heat supplied by the electric resistance, Q_{l1} is the heat loss at the side of the casing, Q_{l2} is the heat loss at the front of the casing and Q_{l3} is the heat loss at the back of the casing.

The heat generated by the electric resistance is calculated as a function of the voltage U and the current I provided by a power supply, as

$$Q_r = U \cdot I \tag{8}$$

The heat loss at the front part depends on the insulation thicknesses E_f of the front surface area A_f, the thermal conductivity of the insulation material k_i and the temperature difference in the insulation wall, as follows:

$$Q_{l2} = \frac{k_i A_f}{E_f}(T_4 - T_5) \tag{9}$$

The heat loss at the lateral surface depends on the length L, the outer and inner radius of the insulation r_e and r_i, the difference in temperature inside and outside the insulation and yields

$$Q_{l1} = \frac{2\pi k_i L}{\left(ln\frac{r_e}{r_i}\right)}(T_3 - T_4). \tag{10}$$

In the back side of the heating system, the heat is lost through the insulation of thickness E_t and area A_b. Furthermore, it depends on temperatures T_1 and T_2, according to

$$Q_{l3} = \frac{k_i A_t}{E_t}(T_2 - T_1). \tag{11}$$

In order to insulate the electric heater, ceramic fiber blanket of density 128 kg/m^3 and thermal conductivity $k_i = 0.140$ W/mK are used [24]. In the back part, the insulation has a thickness of $E_t = 18$ mm and in the front part, where the drill is, the thickness is $E_f = 33$ mm. The total length of the insulation around the electric heater is $L = 59$ mm with an inner radius of $r_i = 42$ mm and outer radius of $r_e = 75$ mm. The power generated by the electric resistance remains constant at $Q_r = 180$ W.

The experimental procedure consists of a heating phase until the temperatures stabilise, followed by application of the cutting fluid. Temperature data are stored in the computer when temperature reaches the steady state, when the thermocouples' variation was less then their resolution. Each experimental run takes about 30 min to reach this condition.

Since the cutting fluids used in abundance are based on water, the experiments are performed using only water. The flow rate of the cutting fluid and rotation speed of the nozzle are the two process variables investigated on the drill temperature and convective coefficient. The cutting fluid is then varied at flow rates of 12, 18 and 24 l/h. The

nozzle rotations are 345, 365 and 385 rpm that are in the range of recommended cutting speeds (21–24 m/s) for machining steel. The drill temperature and convective coefficient of the static nozzle are also performed.

4 Numerical analysis

The part of the drill that is used in the analysis in the temperature simulation is modelled using the opensource CAD software *OnShape*. A mathematical model of the cross-sectional profile of the drill flute is the proposed by [25]. The calculated cross-sectional area of the drill is $A_1 = 132\,\text{mm}^2$ and the lateral surface area of the drill where the cutting fluid acts is $A_2 = 734\,\text{mm}^2$. The CAD model is exported to the software *Salome*, which uses the finite volume mesh generator *NETgen*. Figure 6 shows the discretized model.

The discretized model consists of 1513 nodes and 5104 tetrahedral elements. The software *OpenFoam* is used to import the model. The temperature distribution in the drill is then simulated by applying the *laplacianFoam* solver, which is based on the finite volume technique, to solve the Eq. 1.

The boundary conditions are the heat flux and temperature on the appropriate surfaces, as presented in Eqs. (2), (3) and (4). The simulation results of temperature in the surface of the model are visualised with help of the *ParaView* software.

The mean temperature T_d on the drill surface where the fluid acts is obtained by the numerical integration of the temperature gradient on that surface, dividing the result by the area, according to Eq. (5).

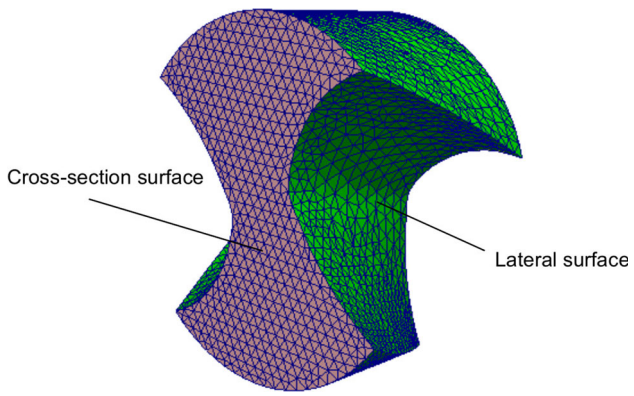

Fig. 6 Discretized of part of the drill corresponding to the control volume VC_1

5 Results and discussions

5.1 Workpiece temperature

The experimental results of the measured temperatures are presented in the Table 1. By analysing the temperatures inside the heating system (T_1 to T_5), it can be noticed that the values did not change significantly as a function of the experimental conditions.

Since the temperatures inside the heating system remain constant, the heat losses and amount of heat entering the drill do not change. The power generated by the electric resistance used in the experiments is $Q_r = 180$ W. The heat lost at the frontal part of the heating system is $Q_{l2} = 12\ W$ (Eq. 9), at the lateral surface is $Q_{l1} = 43$ W (Eq. 10) and at the back part is $Q_{l3} = 10$ W (Eq. 11). Thus, the amount of heat flowing into the drill, calculated using the Eq. (7), is $Q_d = 115$ W.

In relation to the cutting fluid temperatures T_f and the room temperature T_a, they also remain stable during the experiment. However, as expected, the temperature at the back part of the tool T_{b2} changes as a function of the cutting fluid flow rate and the nozzle rotation speed. This occurs because of the action of the cutting fluid, cooling the lateral surface of the drill.

The Fig. 7 shows the temperature at the back part of the tool T_{b2} as a function of the nozzle rotation speed, for a flow rate of 12 l/h. It can be noted that the temperature T_{b2} decreases from 68.1 °C for the static nozzle, stabilising to around 57.0 °C with the increase of R_n.

5.2 Determination of the convective heat transfer coefficient

After the boundary conditions Q_b and T_{b2} are obtained, it is possible to simulate the temperature distribution on the drill surface that is in contact with the cutting fluid.

The heat Q_d enters through the cross-section area A_1 and leaves the drill tool through the side area A_2, which is in contact with the cutting fluid, as presented in Fig. 3, according the boundary conditions established by Eqs. (2), (3) and (4).

The temperature distribution on the helical surface of the drill, resulting from the simulations for the flow rate $l_f = 12$ l/h and rotations speed $R_n = 0$ and $R_n = 385$ rpm is shown in Fig. 8. It is possible to note that, by increasing the nozzle rotation speed, the area of lower temperatures increases and the area of higher temperatures decreases. The highest temperatures are around 145.9 and 134.5°C, and the lowest temperatures are around 52.4° and 41.3°C for $R_n = 0$ rpm and $R_n = 385$ rpm, respectively. Therefore,

Table 1 Measured temperatures for different conditions

T (°C)	Experiment												
	$l = 12$ l/h				$l = 18$ l/h			$l = 24$ l/h			$l = 30$ l/h		
	R_n (rpm)				R_n (rpm)			R_n (rpm)			R_n (rpm)		
	0	345	365	385	345	365	385	345	365	385	345	365	385
T_1	410.5	404.0	402.0	402.0	405.3	407.9	410.6	410.7	408.5	411.1	409.1	409.9	410.6
T_2	652.8	649.8	649.5	651.2	655.9	661.1	663.5	661.3	658.4	669.6	658.5	659.2	661.2
T_3	193.1	189.4	188.0	187.6	188.5	189.1	190.1	190.5	189.1	190.0	192.8	193.4	193.4
T_4	669.1	660.9	659.9	661.7	666.3	670.9	672.9	671.0	668.0	677.7	667.5	669.4	671.0
T_5	118.6	112.0	102.1	100.5	109.0	109.6	109.2	103.5	101.1	100.7	107.2	106.2	105.7
T_{b2}	68.1	61.1	56.6	57.0	54.7	51.2	50.6	47.9	46.7	46.4	46.7	45.5	45.8
T_f	28.0	29.1	29.7	30.0	30.3	30.3	30.2	30.3	30.2	30.2	32.4	31.9	31.9
T_a	23.8	26.0	26.2	26.3	26.3	26.2	26.0	26.0	26.0	25.9	28.4	28.4	28.4

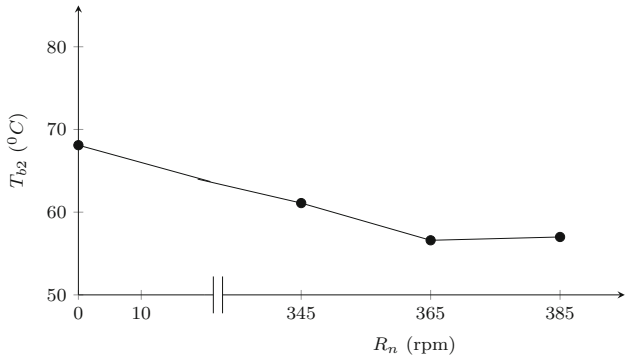

Fig. 7 Temperature at the back part of the tool as a function of the nozzle rotation speed

the temperatures have a decrease of approximately 11°C with the nozzle rotation.

To calculate the mean convective heat transfer coefficient h, it is now necessary to predict the mean temperature T_d on the lateral surface of the drill, with area A_1. The Table 2 shows the results of mean surface temperature, T_d, and the cutting fluid temperature, T_f, both used to calculate h, Eq. (6). It may be noted that, as the flow rate and the nozzle rotation speed increase, the mean temperature on the drill surface T_d decreases.

Figure 9 shows the mean temperature T_d as a function of the flow rate l_f for the different rotation speeds R_n. It is observed that the maximum mean temperature is 79°C for the lower flow rate and slower rotation speed. The values of T_d tend to be around 63 °C regardless of the nozzle rotation speed.

In general, the flow rate leads to the variation in the temperatures at the lateral surface of the drill; larger flow rates give rise to lower temperatures. In relation to the influence of the nozzle rotation speed, it is observed that temperatures for static nozzle are higher than for rotating nozzle. However, only a small influence is observed when the rotation speeds vary between the recommended cutting speeds. The small variation in the nozzle rotation speed contributes very little on the drill temperature.

The difference between the nozzle rotations $R_n = 345$ and $R_n = 365$ rpm of each flow rate also changes. For the flow rate $l_f = 12$ l/h, the difference between them is about

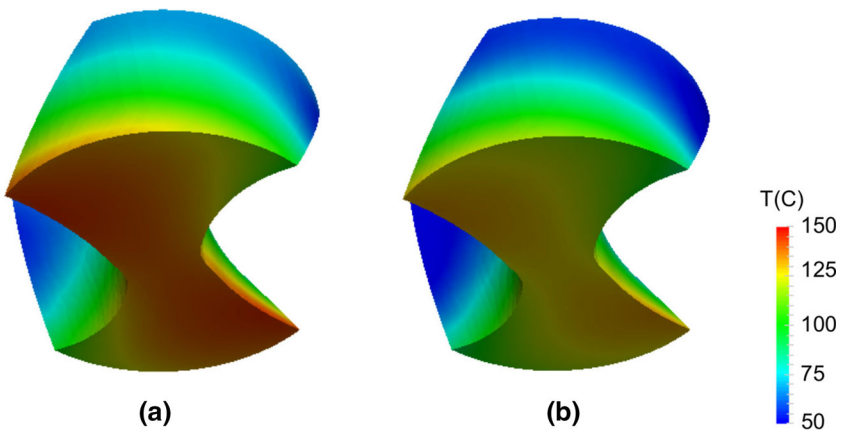

Fig. 8 Simulation of the drill surface temperature for $l_f = 12\ l/h$ e **a** $R_n = 0$ rpm e **b** $R_n = 385$ rpm

Table 2 Calculated results for different conditions

	Experiment												
	$l = 12$ l/h				$l = 18$ l/h			$l = 24$ l/h			$l = 30\ l/h$		
	R_n (rpm)				R_n(rpm)			R_n (rpm)			R_n (rpm)		
	0	345	365	385	345	365	385	345	365	385	345	365	385
T_d (°C)	85.7	78.7	74.2	74.5	72.2	68.6	67.9	65.3	64.1	63.7	64.2	63.0	63.3
T_f (°C)	28.0	29.1	26.7	30.0	30.3	30.3	30.2	30.3	30.2	30.2	32.4	31.9	31.9
$h(\frac{W}{m^2 W})$	2803	3270	3634	3623	3840	4186	4242	4582	4740	4733	5072	5186	5124

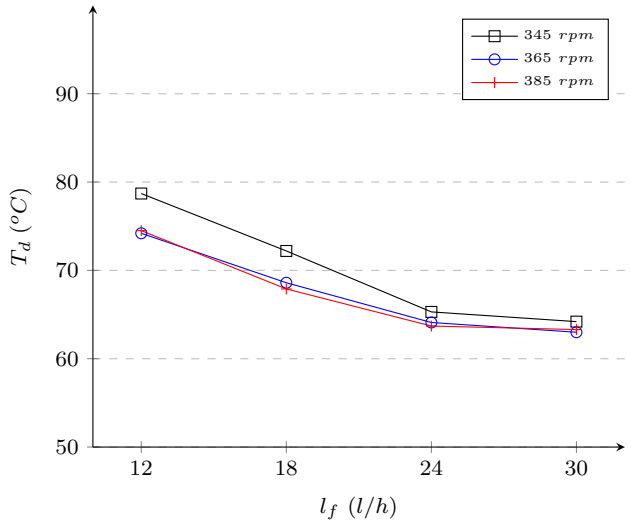

Fig. 9 Mean temperature on the lateral surface of the drill as a function of the fluid flow rate

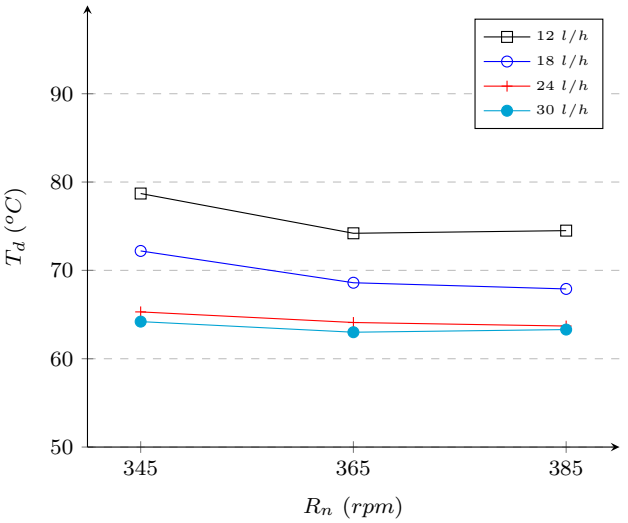

Fig. 10 Mean temperature on the lateral surface of the drill T_d as a function of the nozzle rotation speed R_n for different flow rates l_f

≈ 5 °C, for the flow rate $l_f = 18$ l/h, the difference is about ≈ 3 °C and for the last flow rate $l_f = 24$l/h, the difference decreases to about ≈ 2 °C.

The influence of the nozzle rotation speed on the mean temperature at the lateral surface of the drill is shown in Fig. 10. As can be seen, the rotation speed does not have significant influence for rotations 365 and 385 rpm. The mean temperatures for the flow rates 24 and 30 l/h are very close, regardless the nozzle rotation speed.

The mean convective heat transfer coefficients as a function of the nozzle rotation speed, for the different flow rates of the cutting fluid, are shown in the Fig. 11. It can be observed that, with the increase of the nozzle rotation speed from $R_n = 345$ to $R_n = 365$ rpm, the convective heat transfer coefficient h increases, after that tending to stabilise for the rotation $R_n = 385$ rpm.

Figure 12 presents the mean convective heat transfer coefficient as a function of the flow rate. For the three different nozzle rotation speeds, a linear trend between the mean convective coefficient and the flow rate can be observed. It can also be noted that the results of h for the

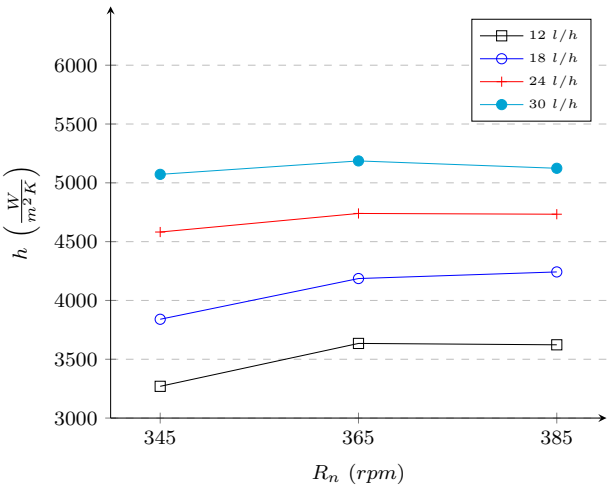

Fig. 11 Convective heat transfer coefficient h as a function of the nozzle rotation speed R_n for different flow rates l_f

rotation speeds $R_n = 365$ and $R_n = 385$ rpm are very close and are higher than for $R_n = 385$ rpm.

The mean convective heat transfer coefficients obtained in this work vary from 3270 W/m^2 K for the flow rate of 12 l/h and rotation $R_n = 345$ rpm to 5190 W/m^2 K for the flow

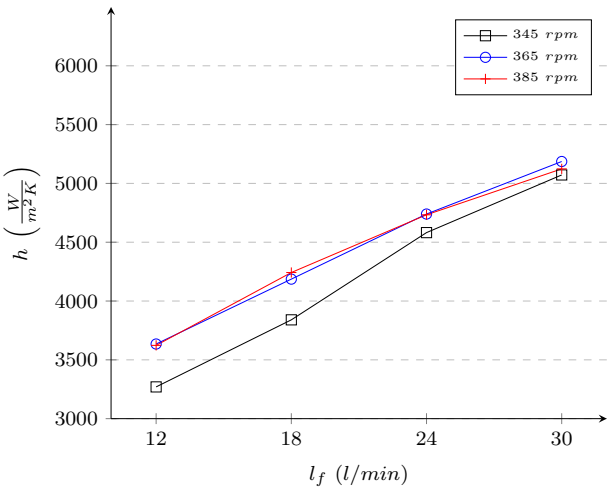

Fig. 12 Convective heat transfer coefficients as a function of the flow rate

of 30 l/h and rotation $R_n = 365$ rpm. When comparing these values with the forced convective heat transfer coefficients (100 to 20,000 W/m^2 K) presented in Bergman et al. [26], it can be noted that they are in a narrow range. In that way, the use of a more real coefficient can increase the prediction accuracy of the temperature at the tool tip and hence the correct amount of cutting fluid.

6 Conclusions

In conventional drilling with helical flutes, the cutting fluid does not reach the chip–tool interface, and, therefore, cooling of the tool body is of fundamental importance. The appropriate rate of the cutting should be determined to maintain the temperature at the tool tip under a certain value in order to minimise the tool wear. For this purpose, the convective heat transfer coefficient between the drill tool body and the cutting fluid must be known. Because of the complex geometry of the drilling tool, the convective heat transfer coefficient has not been explored in the literature. To circumvent this problem, in this work an experimental setup is developed with the purpose of mimicking the rotation of the drill. The tool remains static and the cutting fluid is supplied by a coolant rotating nozzle. This allows the control of the heat flux and measurement of the drill temperature with thermocouple. The verified parameters are the cutting fluid flow rate at values that correspond to a minimum considered as flooding and the coolant nozzle rotation at recommended values according to the cutting speed of the drill tool for machining steel.

According to the results presented in this paper, the following conclusions can be drawn:

- The coolant nozzle rotation has significant effect on the convective heat transfer coefficient compared with the static one.
- No significant influence on the convective heat transfer coefficient is noticed when the coolant nozzle rotation varies between the spindle speed 345 and 385 rpm.
- The fluid flow rate has a significant effect on the convective heat transfer, showing a linear relationship.
- The calculated mean convective heat transfer coefficient varies from 3270 to 5190 W/m^2 K, depending especially on the fluid flow rate.

Thus, these results can be used in a finite element simulation to predict the temperature at the tool tip in the drilling. In this way, the amount of cutting fluid can be optimised to minimise wear of the drill tool.

References

1. Sato M, Aoki T, Tanaka H, Takeda S (2013) Variation of temperature at the bottom surface of a hole during drilling and its effect on tool wear. Int J Mach Tool Manuf 68:40–47
2. Najiha M, Rahman M (2014) A computational fluid dynamics analysis of single and three nozzles minimum quantity lubricant flow for milling. Int J Automot Mech Eng 10(1):1891–1900
3. Obikawa T, Asano Y, Kamata Y (2009) Computer fluid dynamics analysis for efficient spraying of oil mist in finish-turning of Inconel 718. Int J Mach Tool Manuf 49(12):971–978
4. Kurgin S, Dasch JM, Simon DL, Barber GC, Zou Q (2012) Evaluation of the convective heat transfer coefficient for minimum quantity lubrication (MQL). Ind Lubr Tribol 64(6):376–386
5. Dhar N, Islam M, Islam S, Mithu M (2006) The influence of minimum quantity of lubrication (MQL) on cutting temperature, chip and dimensional accuracy in turning AISI-1040 steel. J Mater Process Technol 171(1):93–99
6. Tschätsch H (2010) Applied machining technology. Springer, New York
7. Wakabayashi T (2010) The role of tribology in environmentally friendly MQL machining. Eng J JTEKT 1007E:2–7
8. Karas A, Bouzit M, Belarbi M (2013) Development of a thermal model in the metal cutting process for prediction of temperature distributions at the tool–chip-workpiece interface. J Theor Appl Mech 51(3):553–567
9. Grzesik W, Bartoszuk M, Nieslony P (2004) Finite difference analysis of the thermal behaviour of coated tools in orthogonal cutting of steels. Int J Mach Tool Manuf 44(14):1451–1462
10. Lazoglu I, Altintas Y (2002) Prediction of tool and chip temperature in continuous and interrupted machining. Int J Mach Tool Manuf 42(9):1011–1022
11. Ber A, Goldblatt M (1989) The influence of temperature gradient on cutting tool's life. CIRP Ann Manuf Technnol 38(1):69–73
12. Debnath S, Reddy MM, Yi QS (2014) Environmental friendly cutting fluids and cooling techniques in machining: a review. J Clean Prod 83:33–47
13. Bacci da Silva M, Wallbank J (1998) Lubrication and application method in machining. Ind Lubr Tribol 50(4):149–152

14. Denkena B, Helmecke P, Hülsemeyer L (2014) Energy efficient machining with optimized coolant lubrication flow rates. Proc CIRP 24:25–31
15. Jiang Z, Zhou F, Zhang H, Wang Y, Sutherland JW (2015) Optimization of machining parameters considering minimum cutting fluid consumption. J Clean Prod 108:183–191
16. Li R, Shih AJ (2007) Tool temperature in titanium drilling. J Manuf Sci Eng 129(4):740–749
17. Bono M, Ni J (2006) The location of the maximum temperature on the cutting edges of a drill. Int J Mach Tool Manuf 46(7):901–907
18. Biermann D, Iovkov I (2013) Modeling and simulation of heat input in deep-hole drilling with twist drills and MQL. Proc CIRP 8:88–93
19. Daniel CM, Rao K, Olson WW, Sutherland JW (1996) Effect of cutting fluid properties and application variables on heat transfer in turning and boring operations. In: Proceedings of the JapanUSA symposium on flexible automation, p 1119–1126
20. Kops L, Arenson M (1999) Determination of convective cooling conditions in turning. CIRP Ann Manuf Technol 48(1):47–52
21. Sales W, Guimaraes G, Machado A, Ezugwu E (2002) Cooling ability of cutting fluids and measurement of the chip–tool interface temperatures. Ind Lubr Tribol 54(2):57–68
22. Luchesi VM, Coelho RT (2012) Experimental investigations of heat transfer coefficients of cutting fluids in metal cutting processes: analysis of workpiece phenomena in a given case study. P I Mech Eng B J Eng 226(7):1174–1184
23. Li R, Shih AJ (2007) Spiral point drill temperature and stress in high-throughput drilling of titanium. Int J Mach Tool Manuf 47(12):2005–2017
24. Nutec Ibar Fibras Cermicas Ltda (2016) Main catalogue: blanke insulation of ceramic fiber HP, Revision 5 (In Portuguese), São Paulo
25. Radhakrishnan T, Kawlra R, Wu S (1982) A mathematical model of the grinding wheel profile required for a specific twist drill flute. Int J Mach Tool Des Res 22(4):239–251
26. Bergman TL, Incropera FP, DeWitt DP, Lavine AS (2011) Fundamentals of heat and mass transfer. Wiley, Amsterdam